Supporting Information

Outstanding hydrogen evolution reaction catalyzed by porous nickel diselenide electrocatalysts**

Haiqing Zhou, Fang Yu, Yuanyue Liu, Jingying Sun, Zhuan Zhu, Ran He, Jiming Bao, William A. Goddard III, Shuo Chen*, Zhifeng Ren*

* Correspondence and requests for materials should be addressed to S. C. schen34@uh.edu or Z. F. R. zren@uh.edu.

1. Methods

Material synthesis. The commercially purchased Ni foam was cut into small pieces with an area of 1 cm^2, which were then immersed into the PVP/HAc solution (0.1 g PVP in 5 ml HAc) for several seconds. After drying it slowly, they were placed in the center of a tube furnace, followed by direct selenization at 600 ^oC for 1h in Ar atmosphere with the Se powder placed at the upstream as Se source.

Electrochemical tests. Electrochemical tests were carried out in a N_2-saturated three-electrode system (Gamry, Reference 600),[1,2] where a saturated calomel electrode was used as the reference electrode, a Pt wire as the counter electrode and as-prepared $NiSe_2$ foams directly as the working electrode. To exclude the possible contribution of any Pt contamination to the catalytic performance, we performed similar measurements using a graphite foil (Alfa Aesar) as the counter electrode, and XPS analysis on several positions of the catalyst surface, where no Pt signals are found on post-HER catalysts.

50-100 potential sweeps between 0.07 V to -0.20 V vs. reversible hydrogen electrode (RHE) at a scan rate of 50 mV/s were applied to electrochemically activate the catalysts prior to the HER measurements and for studying the electrochemical stability. The electrochemical impedance spectroscopy curves were collected at a potential of -0.14 V vs. RHE in the same device configuration by tuning the frequency from 10 mHz to 1 MHz with a 10 mV AC dither.

Computational methods. To identify the active site for HER, we performed Density Functional Theory (DFT) calculations using the Vienna Ab-initio Simulation Package (VASP)[3,4] with projector augmented wave (PAW) pseudopotentials[5,6] and the Perdew-Burke-Ernzerhof (PBE) exchange-correlation functional.[7] We used 400 eV for the plane-wave cutoff, and fully relaxed the systems until the final force on each atom is less than 0.01 eV/Å. We have doubled checked the free energies of H adsorption on perfect surface and vacancy-containing surfaces using 500 eV, and found the values differ by < 10 meV. We used a slab of 2×2 surface supercell, with a thickness of 4 stoichiometric layers, and 5×5×1 Monkhorst-Pack k-points sampling.[8] Following the approach of Ref. 9 and 10, the free energy of hydrogen adsorption (ΔG_{H*}) is calculated as $\Delta G_{H*} = E_{ad} + \Delta E_{ZP} + TS$, where E_{ad} is the adsorption energy of H onto the surface, referenced to the 1/2 of energy of the H_2 moleccule (see below), E_{ZP} is the difference in zero point energy between the adsorbed H and the H_2 molecule, T is the room temperature, and S is the 1/2 entropy of H_2 molecule at standard conditions. The adsorption energy E_a is calculated as $E_a = E(\text{H+surface}) - E(\text{surface}) - E(H_2)/2$, where E(H+surface), E(surface) and $E(H_2)$ are the energies of H-adsorbed surface, pure surface, and an H_2 molecule, respectively.

2. SEM morphologies of porous $NiSe_2$ catalyst from original Ni foam

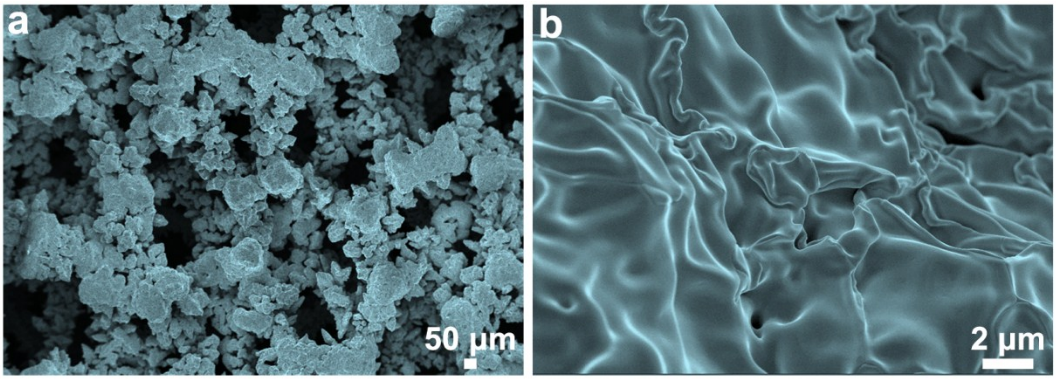

Figure S1. Low and high-magnification SEM images of as-prepared $NiSe_2$ foam from commercial Ni foam without any treatment.

3. Energy dispersive X-ray spectrum (EDS) of as-grown $NiSe_2$ catalyst

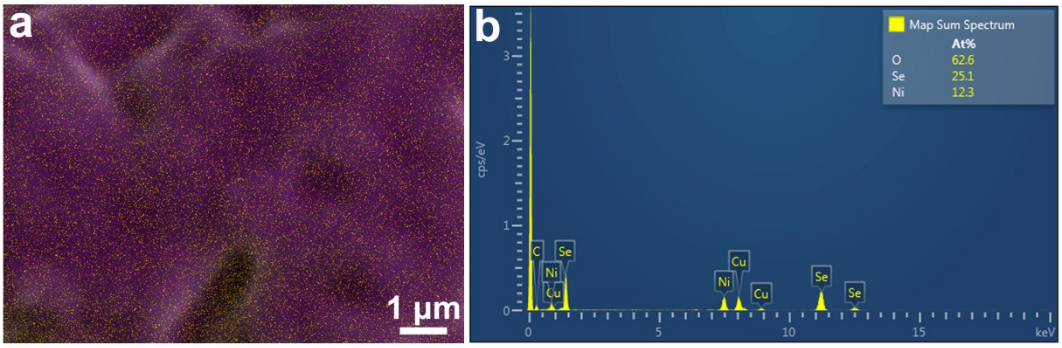

Figure S2. a, Elemental EDS mapping of Ni (yellow) and Se (purple) elements in the same image. **b**, Original EDS analysis on the chemical composition of as-prepared $NiSe_2$ foam from HAc and PVP co-treated Ni foam under TEM.

4. XPS spectra of different as-prepared $NiSe_2$ catalysts

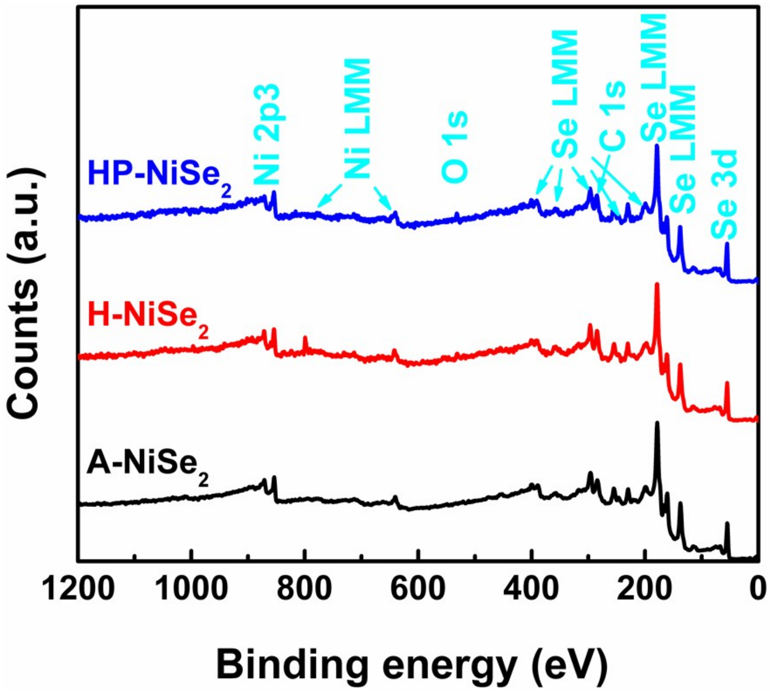

Figure S3. XPS spectra of different $NiSe_2$ foams.

5. **Comparison of the catalytic performance of HP-$NiSe_2$ catalysts between Pt and graphite foil counter electrode**

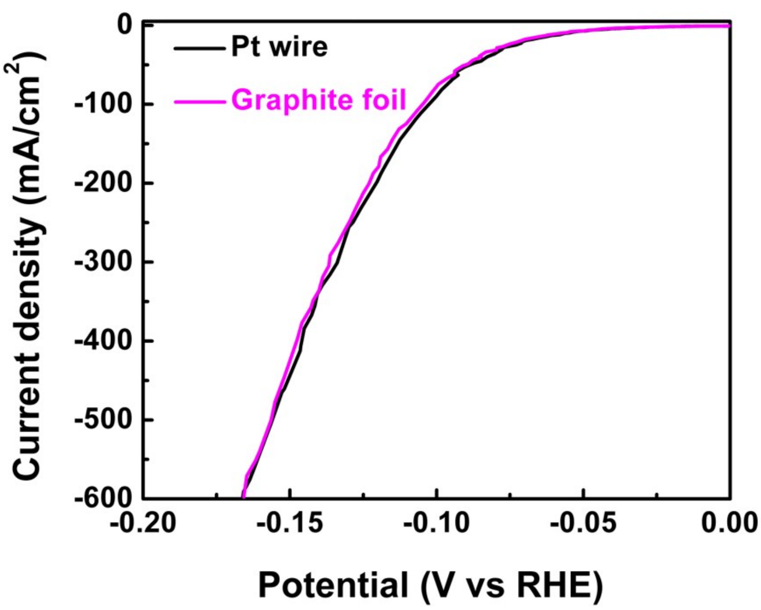

Figure S4. The polarization curves of the HP-$NiSe_2$ catalysts when using Pt or graphite foil as counter electrode. No obvious differences are detected during the measurements.

6. The summary of the catalytic performance for porous $NiSe_2$ catalysts

Table S1. The main performance parameters of different $NiSe_2$ foams in comparison with a Pt wire investigated in Figure 3. Here j_0,η_{10} and η_{100} are corresponding to the exchange current density, the potentials vs RHE at 10 mA cm^{-2}, and 100 mA cm^{-2}, respectively.

Catalyst	Tafel slope	j_0	η_{10}	η_{100}
A-$NiSe_2$	46.0 mV dec^{-1}	8.6 μA cm^{-2}	153 mV	200 mV
H-$NiSe_2$	42.6 mV dec^{-1}	64.6 μA cm^{-2}	107 mV	153 mV
HP-$NiSe_2$	43.0 mV dec^{-1}	612.0 μA cm^{-2}	57 mV	103 mV
Pt wire	31.0 mV dec^{-1}	1126.2 μA cm^{-2}	32 mV	72 mV

7. The comparison of our catalystswith other reported cheap electrocatalysts

Table S2. The comparison on the HER performance of our catalysts with other available cheap HER electrocatalysts in the literatures. These values j_0, η_{10}, and η_{100} represent the exchange current density, the potentials vs RHE at 10 mA/cm^2 and 100 mA/cm^2, respectively.

Catalyst	**Tafel slope**	η_{10}	η_{100}	j_0	**Source**

Benchmark Pt	31.0 mV dec^{-1}	32 mV	72 mV	1126.2 μA cm^{-2}	This work
HP-$NiSe_2$ foam	43.0 $mVdec^{-1}$	57 mV	103 mV	612.0 μA cm^{-2}	This work
$MoS_{2(1-x)}Se_{2x}/NiSe_2$	42.0 $mVdec^{-1}$	69 mV	112 mV	299.4 μA cm^{-2}	2
MoS_x/N-CNT	40 $mVdec^{-1}$	110 mV	225 mV	33.1 μA cm^{-2}	11
$NiSe_2$ nanosheets/CC	32 $mVdec^{-1}$	117 mV	NA	4.7 μA cm^{-2}	12
CoS_2/RGO-CNT	51 $mVdec^{-1}$	142 mV	178 mV	62.6 μA cm^{-2}	13
FeS_2 nanosheets	46 $mVdec^{-1}$	108 mV	170 mV	5.5 μA cm^{-2}	14
$CoSe_2$/carbon fiber	42 $mVdec^{-1}$	139 mV	184 mV	6μA cm^{-2}	15
$WS_{1.56}Se_{0.44}$ nanoribbons	68 $mVdec^{-1}$	176 mV	NA	25 μA cm^{-2}	16
Ni_5P_4-Ni_2P nanosheets	79 $mVdec^{-1}$	120 mV	200 mV	116 μA cm^{-2}	17
Ni_2P nanoparticles	46 $mVdec^{-1}$	105 mV	180 mV	33 μA cm^{-2}	18
CoP nanowire array/CC	51 $mVdec^{-1}$	67 mV	204 mV	288 μA cm^{-2}	19
Mo-W-P nanosheets/CC	52 $mVdec^{-1}$	100 mV	138 mV	288 μA cm^{-2}	20
Metallic WO_2/carbon	46 $mVdec^{-1}$	58 mV	NA	640 μA cm^{-2}	21
MoO_2/PC-RGO	41 $mVdec^{-1}$	64 mV	NA	480 μA cm^{-2}	22
CoPS NPls/carbon paper	56 $mVdec^{-1}$	48 mV	NA	984 μA cm^{-2}	23
CoPS NWs/carbon paper	48 $mVdec^{-1}$	61 mV	NA	554 μA cm^{-2}	23
MoS_2/N-RGO	41.3 $mVdec^{-1}$	56 mV	NA	720 μA cm^{-2}	24

NA: not provided in the data.

8. Double-layer capacitance measurements

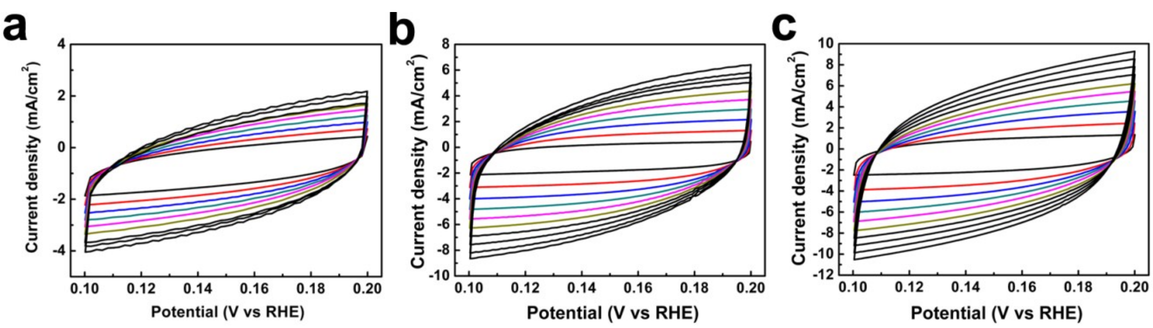

Figure S5. Electrochemical cyclic voltammetry curves of different $NiSe_2$ foams with different scan rates. **a**, A-$NiSe_2$ foam with scan rates ranging from 20 mV/s to 200 mV/s with a step of 20 mV/s. **b**, H-$NiSe_2$ foam with scan rates from 5 mV/s to 50 mV/s with a 5 mV/s interval. **c**, HP-$NiSe_2$ foam with scan rates ranging from 2 mV/s to 20 mV/s with an interval point of 2 mV/s. The potential is scanned from 0.1 to 0.2 V vs RHE where no faradic current was detected.

9. Electrical conductivity measurements of bulk $NiSe_2$ crystals

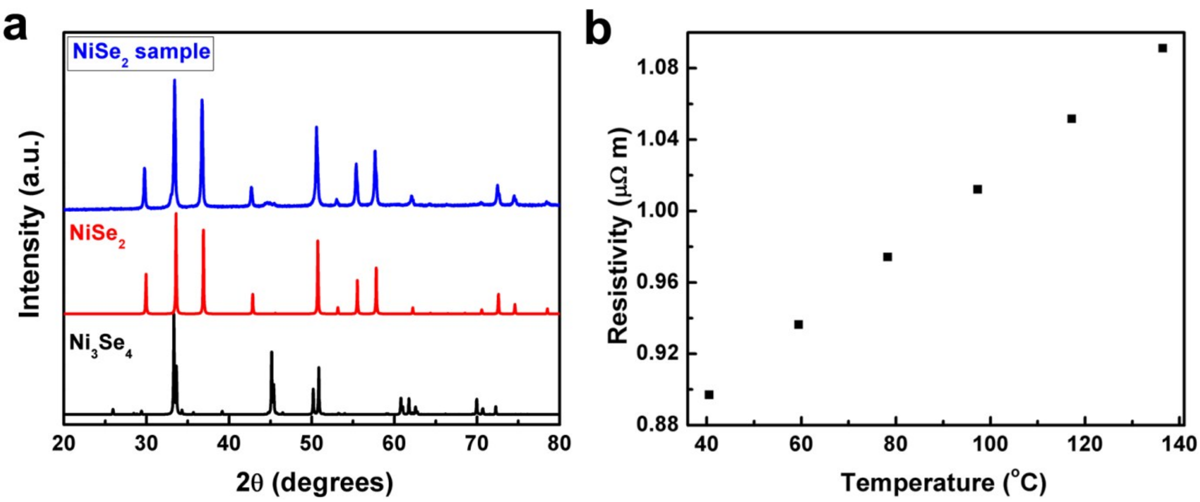

Figure S6. (a) XRD pattern and (b) electrical resistivity measurements of a bulk $NiSe_2$ sample prepared by mechanical alloying of high-purity Ni and Se powders by a high-energy ball mill (SPEX 8000D) for 20 h and hot pressing at 773 K for 2 min.

10. Data for Fig. 4 and structure of the $NiSe_2$ slab (in VASP CONTCAR format)

	perfect	V-Ni	V-Se	V-2Se	ad-Ni	ad-Se	ad-2Se
Free energy(eV/H)	0.68	0.39	0.38	0.47	0.71	0.09	-0.01

```
NiSe2
   1.00000000000000
    11.8719999999999999    0.0000000000000000    0.0000000000000000
     0.0000000000000000   11.8719999999999999    0.0000000000000000
     0.0000000000000000    0.0000000000000000   20.0000000000000000
   Ni   Se
    32    64
Selective dynamics
Direct
  0.0066675993522886 -0.0004355373005453  0.2999600727090445   T   TT
 -0.0001573366221758  0.9964795028284821  0.5978825527890403   T   TT
  0.2499012177917495 -0.0031784384313857  0.4442511860497020   T   TT
0.2567799758378674  0.9986516520039094  0.7421057312696081   T   TT
0.2432973852295297  0.2495747208374209  0.2999697633520752   T   TT
0.2501173976560165  0.2464663422859265  0.5978950253180432   T   TT
0.0000848300246491  0.2468096293625826  0.4442550960502816   T   TT
0.9931873788988308  0.2486366513258388  0.7421053277570332   T   TT
0.0067043028102850  0.4995737853818545  0.2999353701053446   T   TT
 -0.0001298464554059  0.4964721527274584  0.5978796696135562   T   TT
0.2498971985875931  0.4968145778524392  0.4442449734775105   T   TT
0.2568089549908256  0.4986335901639650  0.7420910833837595   T   TT
0.2433021255599140  0.7496188376144860  0.2999641487087098   T   TT
0.2501027529849907  0.7464764389217743  0.5978844609956306   T   TT
0.0000917638536297  0.7468215031264130  0.4442460897100310   T   TT
0.9931762041351612  0.7486665555319038  0.7420949265791846   T   TT
  0.5067064339616435 -0.0004266420373065  0.2999536711075301   T   TT
0.4998460786650789  0.9964652581750038  0.5978864022950832   T   TT
  0.7499102865149861 -0.0031877719648247  0.4442443633147298   T   TT
0.7567804537390733  0.9986501639412766  0.7421033000407599   T   TT
0.7432972336757780  0.2495646864052058  0.2999535705460435   T   TT
0.7501171792452987  0.2464816160993655  0.5978922480052052   T   TT
```

0.5000968095526603	0.2468125008092458	0.4442432347618467	T	TT
0.4931954618372723	0.2486353002224210	0.7421012516904474	T	TT
0.5066639486845046	0.4995791564660371	0.2999554306212046	T	TT
0.4998591017430232	0.4964796890511174	0.5978810304384220	T	TT
0.7499048370558340	0.4968222699209380	0.4442457222550898	T	TT
0.7567820392772402	0.4986481314187219	0.7420953472505711	T	TT
0.7433184301608693	0.7495736242801179	0.2999393646666617	T	TT
0.7501097081881132	0.7464520642833561	0.5978715305711257	T	TT
0.5001204646828332	0.7468298456148145	0.4442425102431442	T	TT
0.4931954578915905	0.7486381865746357	0.7421035469802468	T	TT
0.1907927969786359	0.1880541082591476	0.4117010696567121	T	TT
0.1901240492343139	0.1910094273591115	0.7214824237164089	T	TT
0.0654943068864851	0.3201315201670959	0.2563990355433776	T	TT
0.0616483255181409	0.3089730156614333	0.5607428114751568	T	TT
0.4382734752528953	0.0591782693844061	0.4813546495431387	T	TT
0.4345344224450297	0.0693235887129809	0.7857177870107539	T	TT
0.3098055216515955	0.4418072382557047	0.3206788003882028	T	TT
0.3091934879496128	0.4375878979398209	0.6304944851914969	T	TT
0.3117391337281156	0.3091985459275519	0.4813517223413623	T	TT
0.3154304176215944	0.3193094517882245	0.7857234113765283	T	TT
0.4401632965040815	0.1918024362855373	0.3206766445655260	T	TT
0.4408151279048972	0.1875763918870014	0.6304884411473085	T	TT
0.0591931825569547	0.4380453468232652	0.4116952597259013	T	TT
0.0598582551509802	0.4410091579621155	0.7214731202646336	T	TT
0.1845089154489411	0.0701504821939064	0.2564412920472130	T	TT
0.1883227815738421	0.0589622981282898	0.5607504511263314	T	TT
0.1907845473173868	0.6880422699905895	0.4116918424394442	T	TT
0.1901017132084825	0.6909583376680670	0.7214708668304328	T	TT
0.0655054031783750	0.8201360171669303	0.2564570429851847	T	TT
0.0616281092922571	0.8089659038567116	0.5607537832990638	T	TT
0.4382679532654134	0.5591487870953404	0.4813592356828884	T	TT
0.4345601618797899	0.5693021905892026	0.7857130462359814	T	TT
0.3098389000428427	0.9418020752203080	0.3206971924977297	T	TT
0.3091606441510620	0.9376046176444035	0.6304731045066628	T	TT
0.3117338346394587	0.8091688834998868	0.4813540871290615	T	TT
0.3154175588899016	0.8193016184854949	0.7857164804727512	T	TT
0.4401799252041339	0.6918290029186221	0.3206988409518404	T	TT
0.4407904428212158	0.6875988957005982	0.6304696779245298	T	TT
0.0591888657781381	0.9380713428028414	0.4116970084732689	T	TT
0.0598580685411532	0.9410167134243548	0.7214723815480248	T	TT
0.1845386031740807	0.5701442117764831	0.2564067193881803	T	TT
0.1883295214683958	0.5589669181277239	0.5607573572598141	T	TT
0.6907903039682503	0.1880586417204357	0.4116867631148922	T	TT
0.6901334886223732	0.1909827088446823	0.7214841925142834	T	TT

0.5654844178423125	0.3201250622804722	0.2564049463806853	T	TT
0.5616447910445674	0.3089588160885678	0.5607510506675475	T	TT
0.9382614956887729	0.0591600588299648	0.4813632082713937	T	TT
0.9345704151888586	0.0693059465126342	0.7857099229220765	T	TT
0.8098323496788763	0.4417948675768673	0.3206749013780870	T	TT
0.8092131232492673	0.4375884051035964	0.6304774596008289	T	TT
0.8117227373637743	0.3091650971237694	0.4813512999135273	T	TT
0.8154390960495758	0.3193053949275121	0.7857191884930221	T	TT
0.9401735469030668	0.1918165242740675	0.3206803107843350	T	TT
0.9407802795686209	0.1875980880700108	0.6304705262947893	T	TT
0.5591895258608022	0.4380254619596619	0.4116906921646882	T	TT
0.5598749638151488	0.4409617888717802	0.7214651306412450	T	TT
0.6845155943607977	0.0701521541125364	0.2563890928069552	T	TT
0.6883245108402770	0.0589609389730473	0.5607606985175621	T	TT
0.6907928027439331	0.6880434905669380	0.4116849724032006	T	TT
0.6901220056106002	0.6909645776734742	0.7214729440377659	T	TT
0.5655001000555500	0.8201455096499601	0.2564192727345181	T	TT
0.5616450033776776	0.8089754943179465	0.5607444708306982	T	TT
0.9382712819849818	0.5591628963709566	0.4813532242279144	T	TT
0.9345439569257222	0.5693333761092404	0.7857059193933913	T	TT
0.8098414292983948	0.9417958949554656	0.3206489539350427	T	TT
0.8091619346508335	0.9375940438711092	0.6304768472966098	T	TT
0.8117526509632023	0.8091401843513990	0.4813513926163112	T	TT
0.8154230525620177	0.8193016496835899	0.7857164528301454	T	TT
0.9401905271530422	0.6917975698632581	0.3206757459046545	T	TT
0.9407868164150627	0.6875933064051533	0.6304707395936480	T	TT
0.5592080123492229	0.9380657619104064	0.4116782894191566	T	TT
0.5598618224287812	0.9410138190517696	0.7214843827920081	T	TT
0.6844921077911069	0.5701213795585953	0.2564245044986694	T	TT
0.6883318078720868	0.5589735181576025	0.5607544276187836	T	TT

References:

1 H. Q. Zhou, Y. M. Wang, R. He, F. Yu, J. Y. Sun, F. Wang, Y. C. Lan, Z. F. Ren and S. Chen, *Nano Energy*, 2016, **20**, 29-36.

2 H. Q. Zhou, F. Yu, Y. F. Huang, J. Y. Sun, Z. Zhu, R. J. Nielsen, R. He, J. M. Bao, W. A. Goddard III, S. Chen and Z. F. Ren, *Nat. Commun.*, 2016, **7**, 12765.

3 G. Kresse and J. Hafner, *Phys. Rev. B*, 1993, **47**, 558-561.

4 G. Kresse and J. Furthmüller, *Phys. Rev. B*, 1996, **54**, 11169-11186.

5 G. Kresse and D. Joubert, *Phys. Rev. B*, 1999, **59**, 1758-1775.

6 P. E. Blöchl, *Phys. Rev. B*, 1994, **50**, 17953-17979.

7 J. P. Perdew, K. Burke and M. Ernzerhof, *Phys. Rev. Lett.*, 1996, **77**, 3865-3868.

8 H. J. Monkhorst and J. D. Pack, *Phys. Rev. B*, 1976, **13**, 5188-5192.

9 B. Hinnemann, P. G. Moses, J. Bonde, K. P. Jørgensen, J. H. Nielsen, S. Horch, I. Chorkendorff and J. K. Nørskov, *J. Am. Chem. Soc.*, 2005, **127**, 5308-5309.

10 J. K. Nørskov, T. Bligaard, A. Logadottir, J. R. Kitchin, J. G. Chen, S. Pandelov and U. Stimming, *J. Electrochem. Soc.*, 2005, **152**, J23-J26.

11 D. J. Li, U. N. Maiti, J. Lim, D. S. Choi, W. J. Lee, Y. Oh, G. Y. Lee and S. O. Kim, *Nano Lett.*, 2014, **14**, 1228-1233.

12 F. M. Wang, Y. C. Li, T. A. Shifa, K. L. Liu, F. Wang, Z. X. Wang, P. Xu, Q. S. Wang and J. He, *Angew. Chem. Int. Ed.*, 2016, **55**, 6919-6924.

13 S. J. Peng, L. L. Li, X. P. Han, W. P. Sun, M. Srinivasan, S. G. Mhaisalkar, F. Y. Cheng, Q. Y. Yan, J. Chen and S. Ramakrishna, *Angew. Chem. Int. Ed.*, 2014, **126**, 12802-12807.

14 D. Y. Wang, M. Gong, H. L. Chou, C. J. Pan, H. A. Chen, Y. Wu, M. C. Lin, M. Guan, J. Yang, C. W. Chen, Y. L. Wang, B. J. Hwang, C. C. Chen and H. J. Dai, *J. Am. Chem. Soc.*, 2015, **137**, 1587-1592.

15 D. S. Kong, H. T. Wang, Z. Y. Lu and Y. Cui, *J. Am. Chem. Soc.*, 2014, **136**, 4897-4900.

16 F. M. Wang, J. S. Li, F. Wang, T. A. Shifa, Z. Z. Cheng, Z. X. Wang, K. Xu, X. Y. Zhan, Q. S. Wang, Y. Huang, C. Jiang and J. He, *Adv. Funct. Mater.*, 2015, **25**, 6077-6083.

17 X. G. Wang, Y. V. Kolen’ko, X. Q. Bao, K. Kovnir and L. F. Liu, *Angew. Chem. Int. Ed.*, 2015, **54**, 8188-8192.

18 E. J. Popczun, J. R. McKone, C. G. Read, A. J. Biacchi, A. M. Wiltrout, N. S. Lewis and R. E. Schaak, *J. Am. Chem. Soc.*, 2013, **135**, 9267-9270.

19 J. Q. Tian, Q. Liu, A. M. Asiri and X. P. Sun, *J. Am. Chem. Soc.*, 2014, **136**, 7587-7590.

20 X. D. Wang, Y. F. Xu, H. S. Rao, W. J. Xu, H. Y. Chen, W. X. Zhang, D. B. Kuang and C. Y. Su, *Energy Environ. Sci*., 2016, **9**, 1468-1475.

21 R. Wu, J. F. Zhang, Y. M. Shi, D. L. Liu and B. Zhang, *J. Am. Chem. Soc.,* 2015,**137**, 6983-6986.

22 Y. J. Tang, M. R. Gao, C. H. Liu, S. L. Li, H. L. Jiang, Y. Q. Lan, M. Han and S. H. Yu, *Angew. Chem. Int. Ed.*, 2015, **54**, 12928-12932.

23 M. Cabán-Acevedo, M. L. Stone, J. R. Schmidt, J. G. Thomas, Q. Ding, H. C. Chang, M. L. Tsai, J. H. He and S. Jin, *Nat. Mater.*, 2015, **14**, 1245-1251.

24 Y. J. Tang, Y. Wang, X. L. Wang, S. L. Li, W. Huang, L. Z. Dong, C. H. Liu, Y. F. Li and Y. Q. Lan, *Adv. Energy Mater.*, 2016, **6**, 1600116.